
Conditional independence testing based on a nearest-neighbor estimator of conditional mutual information

Jakob Runge*

Grantham Institute, Imperial College London,
SW72AZ London, United Kingdom

Abstract

Conditional independence testing is a fundamental problem underlying causal discovery and a particularly challenging task in the presence of nonlinear and high-dimensional dependencies. Here a fully non-parametric test for continuous data based on conditional mutual information combined with a local permutation scheme is presented. Through a nearest neighbor approach, the test efficiently adapts also to non-smooth distributions due to strongly nonlinear dependencies. Numerical experiments demonstrate that the test reliably simulates the null distribution even for small sample sizes and with high-dimensional conditioning sets. The test is better calibrated than kernel-based tests utilizing an analytical approximation of the null distribution, especially for non-smooth densities, and reaches the same or higher power levels. Combining the local permutation scheme with the kernel tests leads to better calibration, but suffers in power. For smaller sample sizes and lower dimensions, the test is faster than random fourier feature-based kernel tests if the permutation scheme is (embarrassingly) parallelized, but the runtime increases more sharply with sample size and dimensionality. Thus, more theoretical research to analytically approximate the null distribution and speed up the estimation for larger sample sizes is desirable.

1 Introduction

Conditional independence testing lies at the heart of causal discovery (Spirtes et al., 2000) and at the same time is one of its most challenging tasks. For observed random variables X, Y, Z , measuring that X and Y are independent given Z , denoted as $X \perp\!\!\!\perp Y|Z$, implies that no causal link can exist between X and Y under the relatively weak assumption of *faithfulness* (Spirtes et al., 2000). A finding of conditional independence is then more pertinent to causal discovery than a finding of (conditional) *dependence* from which a causal link only follows under stronger assumptions (Spirtes et al., 2000).

Here we focus on the difficult case of continuous variables (Bergsma, 2004). While various conditional independence (CI) tests exist if assumptions such as linearity or additivity (Daudin, 1980; Peters and Schölkopf, 2014) are justified (for a numerical comparison see Ramsey (2014)), here we focus on the general definition of CI implying that the conditional joint density factorizes: $p(X, Y|Z) = p(X|Z)p(Y|Z)$. Note that wrong assumptions can lead to incorrectly detecting CI (type II error, false negative), but also to wrongly concluding on conditional dependence (type I error, false positive).

Recent research has focused on the general case without assuming a functional form of the dependencies as well as the data distributions. One approach is to discretize the variable Z and make use of easier unconditional independence tests $X \perp\!\!\!\perp Y|Z = z$ (Margaritis, 2005; Huang, 2010). However, this method suffers from the curse of dimensionality for high-dimensional conditioning sets Z .

On the other hand, kernel-based methods are known for their capability to deal with nonlinearity and high dimensions (Fukumizu et al., 2008). A popular test is the Kernel Conditional Independence Test (KCIT)

*Also at: German Aerospace Agency, Institute of Data Science, Jena, Germany.

(Zhang et al., 2012) which essentially tests for zero Hilbert-Schmidt norm of the partial cross-covariance operator, or the Permutation CI test (Doran et al., 2014) which solves an optimization problem to generate a permutation surrogate on which kernel-two sample testing can be applied. Kernel methods suffer from high computational complexity since large kernel matrices have to be computed. Strobl et al. (2017) present two types of orders of magnitude faster CI tests based on approximating kernel methods using *random Fourier features*, called Randomized Conditional Correlation Test (RCoT) and Randomized Conditional Independence Test (RCIT). RCoT can be related to kernelized two-step conditional independence testing (Zhang et al., 2017). Last, Wang et al. (2015) proposed a *conditional distance correlation* (CDC) test based on the correlation of distance matrices between X, Y, Z which have been linked to kernel-based approaches (Sejdinovic et al., 2013).

Kernel methods in general require carefully adjusted bandwidth parameters that characterize the length scales between samples in the different subspaces of X, Y, Z . These bandwidths are *global* in each subspace in the sense that they are applied on the whole range of values for X, Y, Z , respectively.

Testing for independence requires access to the null distribution under CI. Strobl et al. (2017) and Wang et al. (2015) derived asymptotic approximations of the theoretical null distributions, but such approximations only hold for larger sample sizes. The alternative are permutation-based approaches, where the null-distribution is generated by computing the test statistic from a permuted sample.

Our approach to testing CI is founded in an information-theoretic framework. The conditional mutual information (CMI) is zero if and only if $X \perp\!\!\!\perp Y|Z$. While some kernel-based measures can also be related to information-theoretic quantities (see, e.g., Fukumizu et al. (2008)), our approach is to *directly* estimate CMI by combining the well-established Kozachenko-Leonenko k -nearest neighbor estimator (Kozachenko and Leonenko, 1987; Kraskov et al., 2004; Frenzel and Pompe, 2007; Vejmelka and Paluš, 2008; Póczos and Schneider, 2012; Gao et al., 2017) with a nearest-neighbor local permutation scheme. Their main advantage is that nearest-neighbor statistics are *locally adaptive*: The hypercubes around each sample point are smaller where more samples are available. Unfortunately, few theoretical results are available for the complex mutual information estimator. While the Kozachenko-Leonenko estimator is asymptotically unbiased and

consistent (Kozachenko and Leonenko, 1987; Leonenko et al., 2008), the variance and finite sample convergence rates are unknown. Hence, our approach relies on a local permutation test that is also based on nearest neighbors and, hence, data-adaptive.

Our numerical experiments comparing the CMI test with KCIT, RCIT, RCoT, and CDC show that the test reliably simulates the null distribution even for small sample sizes and with high dimensional conditioning sets. The local permutation scheme yields better calibrated tests for sample sizes below 1000 than kernel-based tests relying on asymptotic approximations such as KCIT, RCIT or RCoT. We also tested RCIT and RCoT combined with our local permutation scheme which yields better calibration for smaller sample sizes. The CMI test reaches the same or higher power levels than the other compared approaches, especially for highly nonlinear dependencies. The computational time of both the CMI test and the kernel tests strongly depends on hyperparameters. We found that for smaller samples sizes CMI is faster than RCIT or RCoT by making use of KD-tree neighbor search methods (Maneewongvatana and Mount, 1999), but a major drawback is its computationally expensive permutation scheme making more theoretical research to analytically approximate the null distribution for larger sample sizes desirable. Code for the CMI test is freely available at <https://github.com/jakobrunge/tigramite>.

2 Conditional independence test

2.1 Conditional mutual information

CMI for continuous and possibly multivariate random variables X, Y, Z is defined as

$$\begin{aligned} I_{X;Y|Z} &= \iiint dx dy dz p(x, y, z) \log \frac{p(x, y|z)}{p(x|z) \cdot p(y|z)} \quad (1) \\ &= H_{XZ} + H_{YZ} - H_Z - H_{XYZ}, \quad (2) \end{aligned}$$

where H denotes the Shannon entropy and where we have to assume that the densities $p(\cdot)$ exist. We wish to test the conditional independence hypothesis

$$H_0 : X \perp\!\!\!\perp Y | Z \quad (3)$$

versus the general alternative. From the definition of CMI it is immediately clear that $I_{X;Y|Z} = 0$ if and only if $X \perp\!\!\!\perp Y|Z$, provided that the densities are well-defined. Shannon-type conditional mutual information is theoretically well-founded and its value is well interpretable as the shared information between

X and Y not contained in Z . While this does not immediately matter for a conditional independence test's p -value, causal discovery algorithms often make use of the test statistic's value, for example to sort the order in which conditions are tested. CMI here readily allows for an interpretation in terms of the relative importance of one condition over another. Note that the test statistic values of kernel-based tests typically depend on the chosen kernel.

2.2 Nearest-neighbor CMI estimator

Inspired by Dobrushin (1958), Kozachenko and Leonenko (1987) introduced a class of differential entropy estimators that can be generalized to estimators of conditional mutual information. This class is based on nearest neighbor statistics as further discussed in Kozachenko and Leonenko (1987); Frenzel and Pompe (2007). For a D_X -dimensional random variable X the nearest neighbor entropy estimate is defined as

$$\hat{H}_X = \psi(n) + \frac{1}{n} \sum_{i=1}^n \left[-\psi(k_{X,i}) + \log(\epsilon_i^{D_X}) \right] + \log(V_{D_X}) \quad (4)$$

with the Digamma function as the logarithmic derivative of the Gamma function $\psi(x) = \frac{d}{dx} \ln \Gamma(x)$, sample length n , volume element V depending on the chosen metric, i.e., $V_{D_X} = 2^{D_X}$ for the maximum metric, $V_{D_X} = \pi^{D_X/2} / \Gamma(D_X/2 + 1)$ for Euclidean metric with Gamma function Γ . For every sample with index i , the integer $k_{X,i}$ is the number of points in the D_X -dimensional ball with radius ϵ_i . Formula (4) holds for any ϵ_i and the corresponding $k_{X,i}$, which will be used in the following definition of a CMI estimator. Based on this entropy estimator, Kraskov et al. (2004) derived an estimator for mutual information where the L_∞ -balls with radius ϵ_i are hypercubes. This estimator was generalized to an estimator for CMI first by Frenzel and Pompe (2007) and independently by Vejmelka and Paluš (2008). The CMI estimator is obtained by inserting the entropy estimator Eq. (4) for the different entropies in the definition of CMI in Eq. (2). For all entropy terms H_{XZ} , H_{YZ} , H_Z , H_{XYZ} in Eq. (2), we use the maximum norm and choose as the side length $2\epsilon_i$ of the hypercube the distance ϵ_i to the $k = k_{XYZ,i}$ -nearest neighbor in the joint space $\mathcal{X} \otimes \mathcal{Y} \otimes \mathcal{Z}$. The

CMI estimate then is

$$\begin{aligned} \hat{I}_{XY|Z} &= \psi(k) + \frac{1}{n} \sum_{i=1}^n [\psi(k_{Z,i}) - \psi(k_{XZ,i}) - \psi(k_{YZ,i})]. \end{aligned} \quad (5)$$

The only free parameter k is the number of nearest neighbors in the joint space of $\mathcal{X} \otimes \mathcal{Y} \otimes \mathcal{Z}$ and $k_{xz,i}$, $k_{yz,i}$ and $k_{z,i}$ are computed as follows for every sample point indexed by i :

1. Determine (here in maximum norm) the distance ϵ_i to its k -th nearest neighbor (excluding the reference point which is not a neighbor of itself) in the joint space $\mathcal{X} \otimes \mathcal{Y} \otimes \mathcal{Z}$.
2. Count the number of points with distance strictly smaller than ϵ_i (including the reference point at i) in the subspace $\mathcal{X} \otimes \mathcal{Z}$ to get $k_{xz,i}$, in the subspace $\mathcal{Y} \otimes \mathcal{Z}$ to get $k_{yz,i}$, and in the subspace \mathcal{Z} to get $k_{z,i}$.

Similar estimators, but for the more general class of Rényi entropies and divergences, were developed in Wang et al. (2009); Póczos and Schneider (2012). Estimator (5) uses the approximation that the densities are constant within the epsilon environment. Therefore, the estimator's bias will grow with k since larger k lead to larger ϵ -balls where the assumption of constant density is more likely violated. The variance, on the other hand, is the more important quantity in conditional independence testing and it becomes smaller for larger k because fluctuations in the ϵ -balls average out. The decisive advantage of this estimator compared to fixed bandwidth approaches is its *data-adaptiveness* (Fig. 1B).

The Kozachenko-Leonenko estimator is asymptotically unbiased and consistent (Kozachenko and Leonenko, 1987; Leonenko et al., 2008). Unfortunately, at present there are no results, neither exact nor asymptotically, on the distribution of the estimator as needed to derive analytical significance bounds. In Goria and Leonenko (2005), some numerical experiments indicate that for many distributions of X , Y the asymptotic distribution of MI is Gaussian. But the important finite size dependence on the dimensions D_X , D_Y , D_Z , the sample length n and the parameter k are unknown.

Some notes on the implementation: Before estimating CMI, we rank-transform the samples individually in each dimension: Firstly, to avoid points with equal distance, small amplitude random noise is added

to break ties. Then, for all n values x_1, \dots, x_n , we replace x_i with the transformed value r , where r is defined such that x_i is the r th largest among all x values. The main computational cost comes from searching nearest neighbors in the high dimensional subspaces which we speed up using *KD-tree* neighbor search (Maneewongvatana and Mount, 1999). Hence, the computational complexity will typically scale less than quadratically with the sample size. Kernel methods, on the other hand, typically scale worse than quadratically in sample size if they are not based on Kernel approximations such as via random Fourier features (Strobl et al., 2017). Further, the CMI estimator scales roughly linearly in k and D , the total dimension of X, Y, Z .

2.3 Nearest-neighbor permutation test

Algorithm 1 Algorithm to generate a nearest-neighbor permutation $\pi(\cdot)$ of $\{0, 1, \dots, n\}$.

- 1: Denote by $d_i^{k_{\text{perm}}}$ the distance of sample point z_i to its k_{perm} -nearest neighbor (including i itself, i.e., $d_i^{k_{\text{perm}}=1} = 0$)
 - 2: Compute list of nearest neighbors for each sample point: $\mathcal{N}_i = \{l \in \{0, \dots, n\} : \|z_l - z_i\| \leq d_i^{k_{\text{perm}}}\}$ with KD-tree algorithm in maximum norm of subspace Z
 - 3: Shuffle \mathcal{N}_i for each i
 - 4: Initialize empty list $\mathcal{U} = \{\}$ of used indices
 - 5: **for all** $i \in$ random permutation of $\{1, \dots, n\}$ **do**
 - 6: $j = \mathcal{N}_i(0)$
 - 7: $m = 0$
 - 8: **while** $j \in \mathcal{U}$ and $m < k_{\text{perm}} - 1$ **do**
 - 9: $m = m + 1$
 - 10: $j = \mathcal{N}_i(m)$
 - 11: $\pi(i) = j$
 - 12: Add j to \mathcal{U}
 - 13: **return** $\{\pi(1), \dots, \pi(n)\}$
-

Since no theory on finite sample behavior of the CMI estimator is available, we resort to a permutation-based generation of the distribution under H_0 .

Typically in CMI-based independence testing, CMI-surrogates to simulate independence are generated by randomly permuting *all* values in X . The problem is, that this approach not only destroys the dependence between X and Y , as desired, but also destroys all dependence between X and Z . Hence, this approach does not actually test $X \perp\!\!\!\perp Y \mid Z$. In order to preserve the dependence between X and Z , we propose a local permutation test utilizing nearest-neighbor search. To avoid confusion, we denote the CMI-

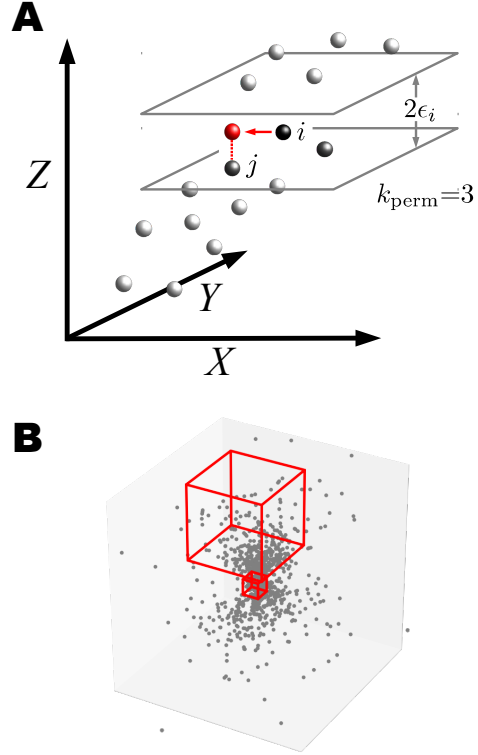


Figure 1: (A) Schematic of local permutation scheme. Each sample point i 's x -value is mapped randomly to one of its k_{perm} -nearest neighbors in subspace Z . The hypercubes with length scale ϵ_i locally adapt to the density making this scheme more data efficient than fixed bandwidth techniques. By keeping track of already ‘used’ indices j , we approximately achieve a random draw *without* replacement, see Algorithm 1. (B) The CMIknn estimator and the local permutation test are data-adaptive: The hypercubes around each sample point are smaller where more samples are available.

estimation parameter as k_{CMI} and the permutation-parameter as k_{perm} .

As illustrated in Fig. 1, we first identify the k_{perm} -nearest neighbors around each sample point i (here including the point itself) in the subspace of Z using the maximum norm. With Algorithm 1 we generate a permutation mapping $\pi : \{1, \dots, n\} \rightarrow \{\pi(1), \dots, \pi(n)\}$ which tries to achieve draws *without* replacement. Since this is not always possible, some values might occur more than once, i.e., they were drawn *with* replacement as in a bootstrap. In Paparoditis and Politis (2000) a bootstrap scheme that *always* draws with replacement is described which is used for the CDC independence test. The difference to our scheme is that we try to avoid tied samples as much as possible

to preserve the conditional marginals.

The permutation test is then as follows:

1. Generate a random permutation $x_b^* = \{x_{\pi_b(1)}, \dots, x_{\pi_b(n)}\}$ with Algorithm 1
2. Compute CMI $\hat{I}(x_b^*; y|z)$ via Eq. (5)
3. Repeat steps (1) and (2) B times, sort the estimates \hat{I}_b from the null and obtain p -value by

$$p = \frac{1}{B} \sum_{b=1}^B \mathbb{1}_{\hat{I}_b \geq \hat{I}(x; y|z)}, \quad (6)$$

where $\mathbb{1}$ denotes the indicator function and $\hat{I}(x; y|z)$ is the CMI estimate of the original data.

The CMI estimator holds for arbitrary dimensions of all arguments X, Y, Z and also the local permutation scheme can be used to jointly permute all of X 's dimensions. In the following numerical experiments, we focus on the case of univariate X and Y and univariate or multivariate Z .

3 Experiments

3.1 Choosing k_{CMI} and k_{perm}

Our approach has two free parameters k_{CMI} and k_{perm} . The following numerical experiments indicate that restricting k_{perm} to only very few nearest neighbors already suffices to reliably simulate the null distribution in most cases while for k_{CMI} we derive a rule-of-thumb based on the sample size n .

Figure 2 illustrates the effect of different k_{perm} . If k_{perm} is too large or even $k_{\text{perm}} = n$, i.e., a full non-local permutation, the permuted distribution under independence (red) is negatively biased. As illustrated by the red markers, this would lead to an increase of false positives (type-I error). On the other hand, for the dependent case, if $k_{\text{perm}} = 1..3$, the permuted distribution is positively biased yielding lower power (type-II errors). For a range of optimal values of k_{perm} , the permuted distribution perfectly simulates the true null distribution.

To evaluate the effect of k_{CMI} and k_{perm} numerically, we followed the post-nonlinear noise model described in Zhang et al. (2012); Strobl et al. (2017) given by $X = g_X(\epsilon_X + \frac{1}{D_Z} \sum_i^{D_Z} Z_i)$, $Y = g_Y(\epsilon_Y + \frac{1}{D_Z} \sum_i^{D_Z} Z_i)$, where $Z_i, \epsilon_X, \epsilon_Y$ have jointly independent standard Gaussian distributions, and

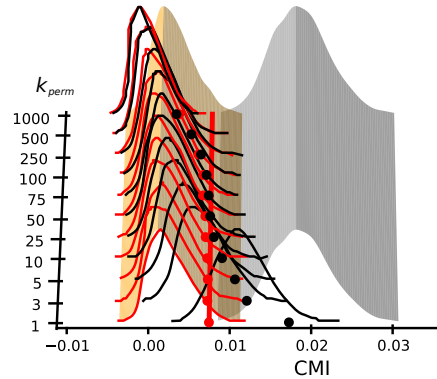


Figure 2: Illustrative simulation of multivariate Gaussian to demonstrate the effect of the nearest-neighbor permutation parameter k_{perm} . The true null distribution of CMI is depicted as the orange surface with the 5% quantile marked by a red straight line, and the true distribution under dependence is drawn as a grey surface (both are constant for all k_{perm}). The red and black distributions and markers give the permuted null distributions and their 5% quantiles for different k_{perm} for the independent (red) and dependent (black) case, respectively. Here the sample size is $n = 1000$ such that $k_{\text{perm}} = 1000$ corresponds to a full non-local permutation.

g_X, g_Y denote smooth functions uniformly chosen from $(\cdot), (\cdot)^2, (\cdot)^3, \tanh(\cdot), \exp(\|\cdot\|^2)$. Thus, we have $X \perp\!\!\!\perp Y | Z = (Z_1, Z_2, \dots)$ in any case. To simulate dependent X and Y , we used $X = g_X(c\epsilon_b + \epsilon_X)$, $Y = g_Y(c\epsilon_b + \epsilon_Y)$ for $c > 0$ and identical Gaussian noise ϵ_b and keep Z independent of X and Y .

In Fig. 3, we show results for sample size $n = 1000$. The null distribution was generated with $B = 1000$ surrogates in all experiments. The results demonstrate that a value $k_{\text{perm}} \approx 5..10$ yields well-calibrated tests while not affecting power much. This holds for a wide range of sample sizes as shown in Fig. 12.

Larger k_{CMI} yield more power and even for $k_{\text{CMI}} \approx n/2$ the tests are still well calibrated. But power peaks at some value of k_{CMI} and slowly decreases for too large values. Still, the dependency of power on k_{CMI} is relatively robust and we suggest a rule-of-thumb of $k_{\text{CMI}} \approx 0.1..0.2n$. Note that, as shown in Fig. 4, runtime increases linearly with k_{CMI} while k_{perm} does not impact runtime much. Here we depict the runtime per CMI estimate assuming that the permutation scheme is (embarrassingly) parallelized.

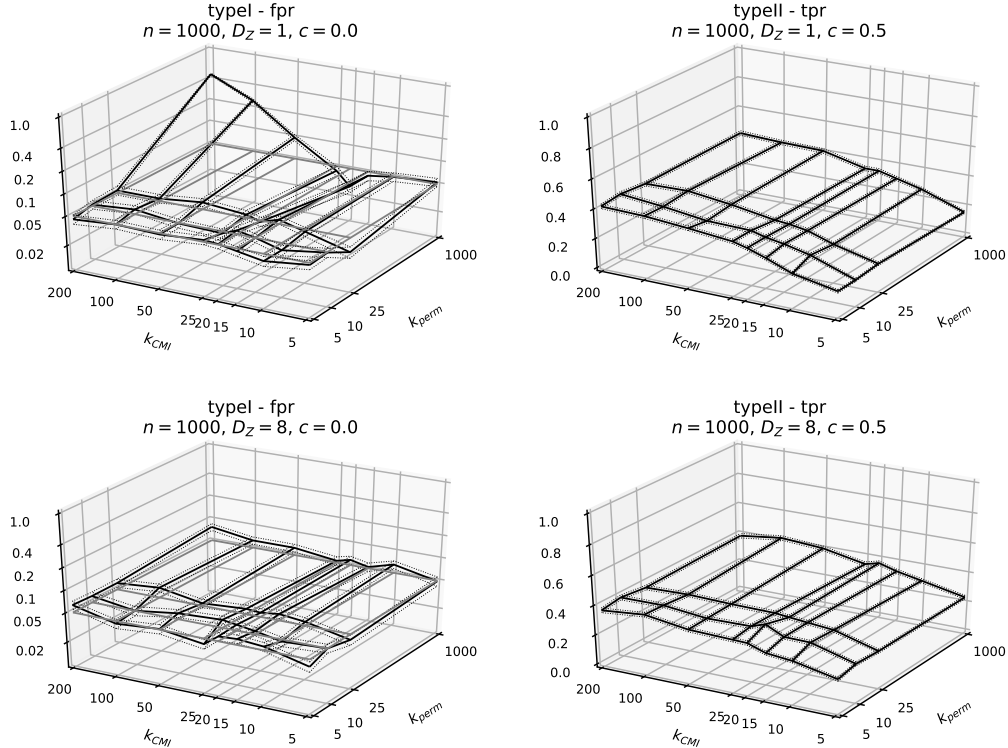


Figure 3: Numerical experiments with post-nonlinear noise model (Zhang et al., 2012; Strobl et al., 2017). The sample size is $n = 1000$ and 1000 realizations were generated to evaluate false positives (FPR) and true positives (TPR) for $c = 0.5$ at the 5% significance level. Shown are FPR and TPR for $D_Z = 1$ (top panels) and $D_Z = 8$ (bottom panels).

3.2 Comparison with kernel measures

In Fig. 5 we show results comparing our CMI test (CMIknn) to KCIT and the two random-fourier-based approximations RCIT and RCoT introduced in Strobl et al. (2017). As a metric for type-I errors, as in Strobl et al. (2017) we evaluated the Kolmogorov-Smirnov (KS) statistic to quantify how uniform the distribution of p -values is. For type-II errors we measure the area under the power curve (AUPC). All metrics were evaluated from 1000 realizations and error bars give the bootstrapped standard errors. We show results for CMIknn for $k_{\text{perm}} = 5$ with $B = 1000$ permutation surrogates and using the rule-of-thumb $k_{\text{CMI}} = 0.2n$ as well as a fixed $k_{\text{CMI}} = 50$.

Figure 5 demonstrates that CMIknn is better calibrated with the lowest KS-values for almost all sample sizes tested. KCIT and RCIT are especially badly calibrated for smaller sample sizes or higher dimensions D_Z and RCoT better approximates the null distribution only for $n \geq 500$ for $D_Z = 1$ and for $n \geq 1000$ for $D_Z = 8$. Note that this is also expected (Strobl et al., 2017) since the analytical approxima-

tion of the null distribution for RCIT and RCoT requires large sample sizes. The power as measured by AUPC is, thus only comparable for $n > 500$ for $D_Z = 1$ and CMIknn has the highest power throughout if k_{CMI} is scaled with the sample size. Also for fixed $k_{\text{CMI}} = 50$ the power of CMIknn is competitive. Also for $D_Z = 8$ and $n \geq 1000$ CMIknn has slightly higher power than RCoT and RCIT.

If the computationally expensive permutation scheme of CMIknn is (embarrassingly) parallelized, the CMIknn test is faster than RCIT or RCoT for not too large sample sizes due to efficient KD-tree nearest-neighbor search procedures (Maneewongvatana and Mount, 1999), especially for smaller k_{CMI} . KCI is not shown here because it is orders of magnitude slower. A major computational burden of RCIT and RCoT is the kernel bandwidth computation via the median Euclidean distance heuristic. In <https://github.com/ericstrobl/RCIT> the median is computed from the first 500 samples only, leading to the “kink” in the runtime for RCIT and RCoT. The runtime of RCIT and RCoT depends quadratically on the number of random Fourier fea-

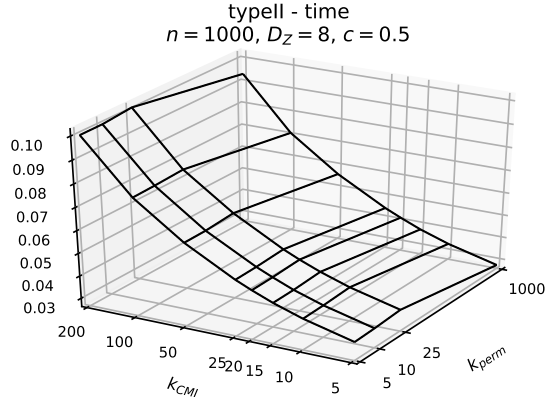


Figure 4: Runtime per estimate [in s] for the same setup as in the lower panels of Fig. 3. For $k_{\text{perm}} = n$ a computationally cheaper full permutation scheme was used.

tures used (here the default of 25 for subspace \mathcal{Z} and 5 for subspaces \mathcal{X} and \mathcal{Y} was used), for more results see Fig. 8. CMIknn’s runtime increases more sharply with sample size.

Our results indicate that the analytical approximations of the null distribution utilized in RCIT and RCoT do not work well for small sample sizes below $n \approx 1000$. In Fig. 6 we explore the option to combine the kernel statistics with our nearest-neighbor permutation test. While then RCIT and RCoT lose their computational advantage, the tests are now well-calibrated. Their power is still mostly lower than that of CMIknn, especially for RCIT.

In Fig. 7 we explore more cardinalities of the conditioning set. KCI and RCIT are not well-calibrated for higher dimensions and also the permutation-version of RCIT quickly loses power for higher dimensions. The power of CMIknn and RCoT is rather insensitive to the dimensionality. Note, however, that in the numerical experiments of Strobl et al. (2017) the conditioning variables Z for evaluating power are independent of X and Y . Other experimental setups might induce a dependence of power on D_Z . CMIknn’s runtime starts lower, but increases more sharply with D_Z than RCIT and RCoT.

Until now we considered rather smooth dependencies of X and Y on the conditioning variables. In Figs. 9,10 we consider more nonlinear relationships. For an extremely oscillatory sinusoidal dependency like $X = \sin(\lambda Z) + \epsilon_X$ and $Y = \sin(\lambda Z) + \epsilon_Y$ ($c\epsilon_b$ added for the dependent case), shown in Fig. 9, k_{perm} needs to be set to a very small value in order

to control false positives. Here the analytical versions of RCIT and RCoT do not work at all and the permutation-based versions have much lower power than CMIknn.

In Fig. 10 we consider a multiplicative noise case with the model $X = g_X(0.1\epsilon'_X + \epsilon_X \frac{1}{D_Z} \sum_i^{D_Z} Z_i)$, $Y = g_Y(0.1\epsilon'_Y + \epsilon_Y \frac{1}{D_Z} \sum_i^{D_Z} Z_i)$ with all variables as before and $\epsilon'_{X,Y}$ another independent Gaussian noise term. For the dependent case we used $X = g_X(c\epsilon_b\epsilon_X)$, $Y = g_Y(c\epsilon_b\epsilon_Y)$ for $c > 0$ and identical Gaussian noise ϵ_b and keep Z independent of X and Y . Even though the density is highly localized in this case, CMIknn is still well calibrated for $k_{\text{perm}} \approx 5$. On the other hand, RCoT cannot control false positives even if we vary the number of Fourier features to much higher values (which takes much longer). RCIT is slightly better suited here, but only combined with the local permutation test both become better calibrated. CMIknn has higher power than both permutation-based kernel tests in this example.

3.3 Comparison with conditional distance correlation

In Tab. 1 we repeat the results from Wang et al. (2015) proposing the CDC test together with results from RCoT and our CMI test. The experiments are described in Wang et al. (2015). Examples 1–4 correspond to conditional independence and Examples 5–8 to dependent cases. CMIknn has well-calibrated tests except for Example 4 (as well as Example 8) which is based on discrete Bernoulli random variables while the CMI test is designed for continuous variables. For Examples 5–8 CMIknn has competitive power compared to CDC and outperforms KCIT in all and RCoT in all but Example 5 where they reach the same performance. Note that the CDC test also is based on a computationally expensive local permutation scheme since the asymptotics break down for small sample sizes.

4 Real data application

We apply CMIknn in a time series version of the PC causal discovery algorithm (Runge et al., 2017) to investigate dependencies between hourly averaged concentrations for carbon monoxide (CO), benzene (C6H6), total nitrogen oxides (NOx), nitrogen dioxide (NO2), as well as temperature (T), relative humidity (RH) and absolute humidity (AH) taken from De Vito et al. (2008)¹. The time series were detrended

¹<http://archive.ics.uci.edu/ml/datasets/Air+Quality>

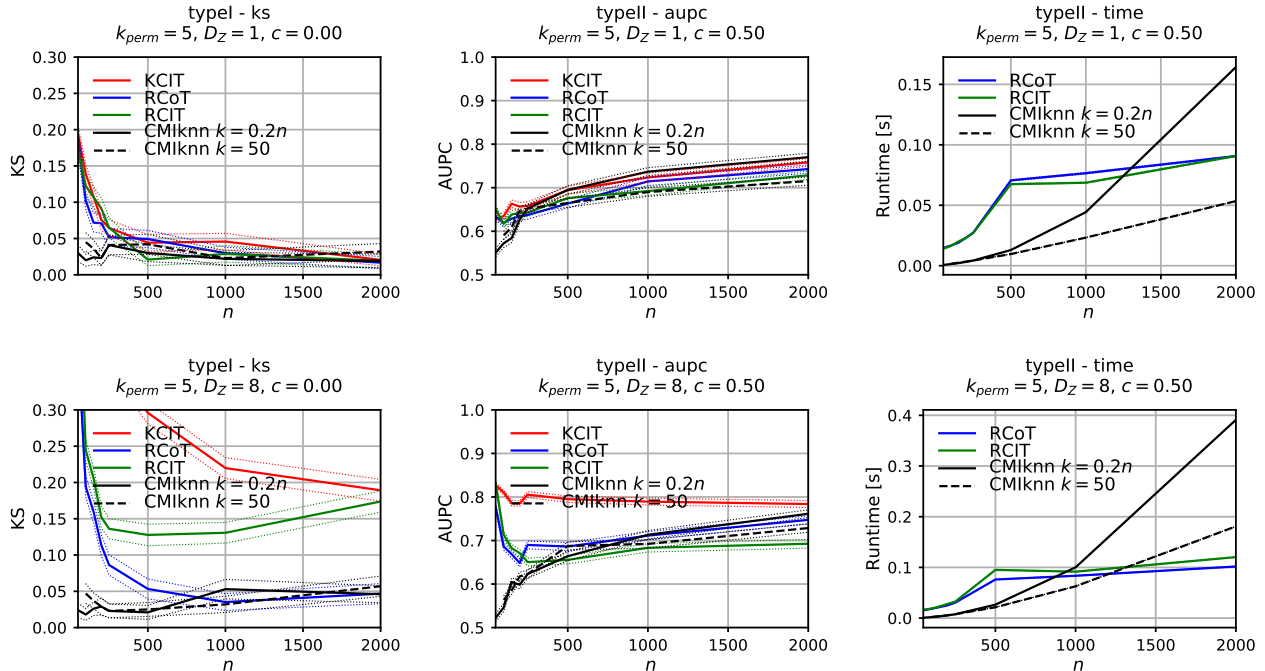


Figure 5: Numerical experiments with post-nonlinear noise model and similar setup as in Strobl et al. (2017). Shown are KS (left column), AUPC (center column), and runtime (right column) for a sample size experiment with $D_Z = 1$ (top row) and $D_Z = 8$ (center row). In all experiments we set $k_{\text{perm}} = 5$ and depict $k_{\text{CMI}} = 0.2n$ and $k_{\text{CMI}} = 50$. Here we show results for the default $n_{\text{ff}} = 25$ fourier features for RCIT and RCoT, but much more are needed to resolve less smooth densities (Figs. 9,10). In Fig. 8 we show more parameter studies for RCIT and RCoT.

using a Gaussian kernel smoother with bandwidth $\sigma = 1440$ hours and we limited the analysis to the first three months of the dataset (2160 samples). After accounting for missing values we obtain an effective sample size of $n = 1102$. As in our numerical experiments, we used the CMiknn parameters $k_{\text{CMI}} = 200$ and $k_{\text{perm}} = 5$ with $B = 1000$ permutation surrogates. The causal discovery algorithm was run including lags from $\tau = 1$ up to $\tau_{\text{max}} = 3$ hours. The resulting graph at a 10% FDR-level shown in Fig. 11 indicates that temperature and relative humidity influence Benzene which in turn affects NO2 and CO concentrations.

5 Conclusion

We presented a novel fully non-parametric conditional independence test based on a nearest neighbor estimator of conditional mutual information. Its main advantage lies in the ability to adapt to highly localized densities due to nonlinear dependencies even in higher dimensions. This feature results in well-calibrated tests with reliable false positive rates. We tested setups for sample sizes $n = 50$ to $n = 2000$

and dimensions of the conditional set of $D_Z = 1..10$. The power of CMiknn is comparable or higher than advanced kernel based tests such as KCIT or its faster random Fourier feature versions RCIT and RCoT, which, however, are not well-calibrated in the smaller sample limit. Combining our local permutation scheme with kernel tests leads to better calibration, but power is still lower than CMiknn. CMiknn has a shorter runtime for not too large sample sizes since efficient nearest-neighbor search schemes can be utilized, but its runtime increases more sharply with sample size and dimensionality than the fourier-feature bases kernel tests. Here approximate nearest-neighbor techniques could speed up computations. The permutation scheme leads to a higher computational load which, however, can be easily parallelized. Nevertheless, more theoretical research is desirable to obtain approximate analytics for the null distribution in the large sample limit. For small sample sizes below $n \approx 1000$ we find that a permutation-approach is inevitable also for kernel-based approaches.

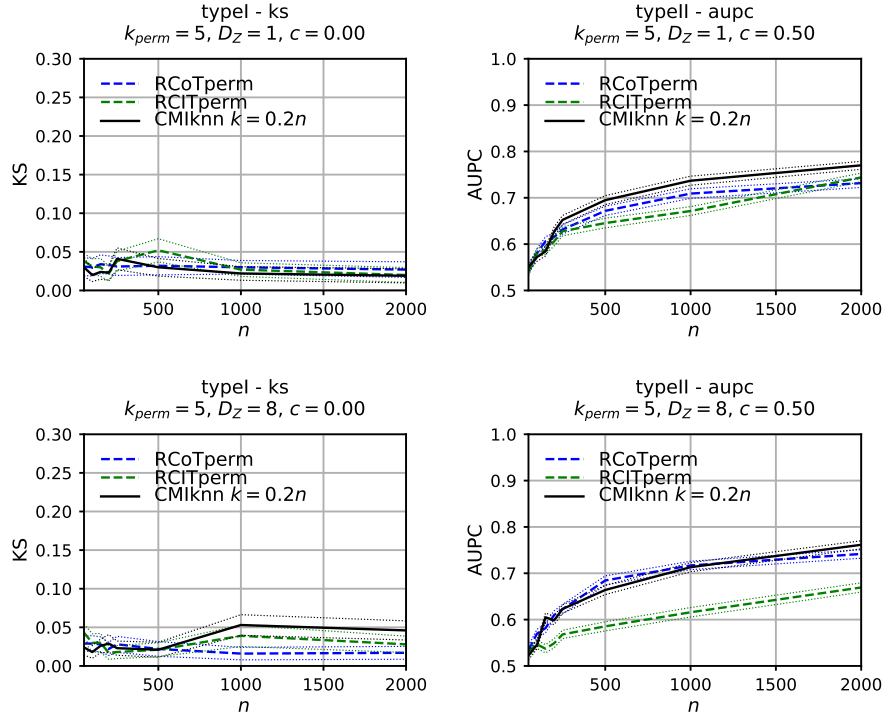


Figure 6: Numerical experiments as before for the kernel measures combined with the proposed nearest-neighbor permutation test with $k_{perm} = 5$.

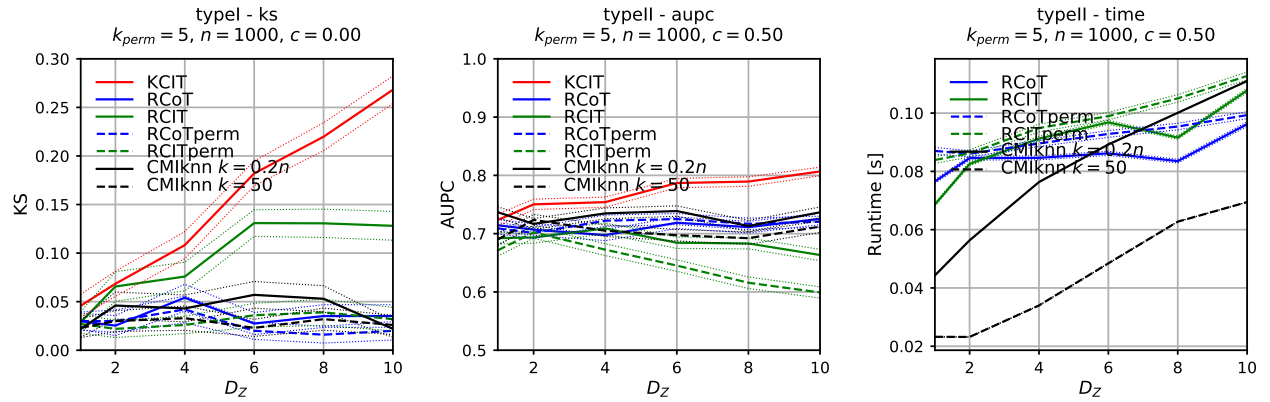


Figure 7: Numerical experiments as before for different condition dimensions D_Z with fixed $n = 1000$.

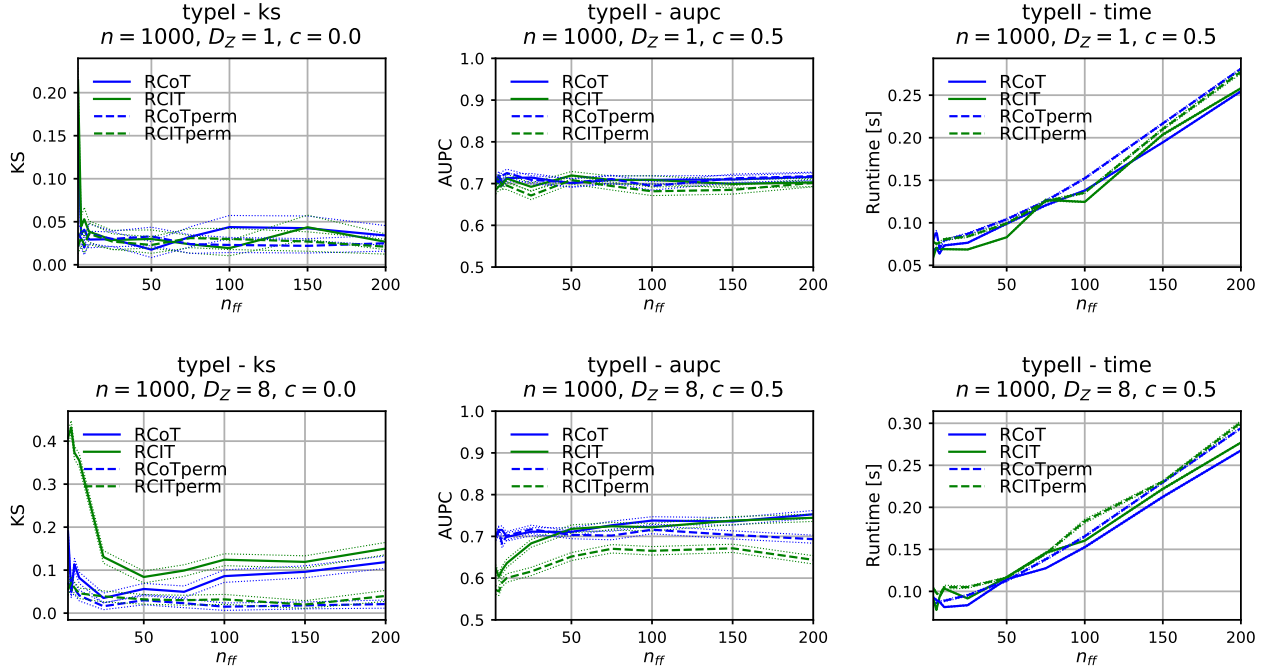


Figure 8: Choice of number of fourier features (n_{ff}) for random fourier-feature based kernel-measures. Experiments based on post-nonlinear noise model and similar setup as in Strobl et al. (2017). Shown are KS (left column), AUPC (center column), and runtime (right column) for a sample size experiment with $D_Z = 1$ (top row) and $D_Z = 8$ (center row). n_{ff} corresponds to the number of features in subspace Z , the number of fourier features in subspaces X and Y is fixed to 5 as implemented in <https://github.com/ericstrobl/RCIT>. Solid lines mark RCIT and RCoT tests based on analytically approximating the null distribution while dashed lines are based on the nearest-neighbor local permutation scheme introduced in this work. While for $D_Z = 1$ $n_{ff} > 10$ yields similar results, for $D_Z = 8$ the KS metric is more sensitive to the choice of n_{ff} , at least for the analytical RCIT and RCoT versions. The runtime of RCIT and RCoT scales roughly quadratically in the number of fourier features.

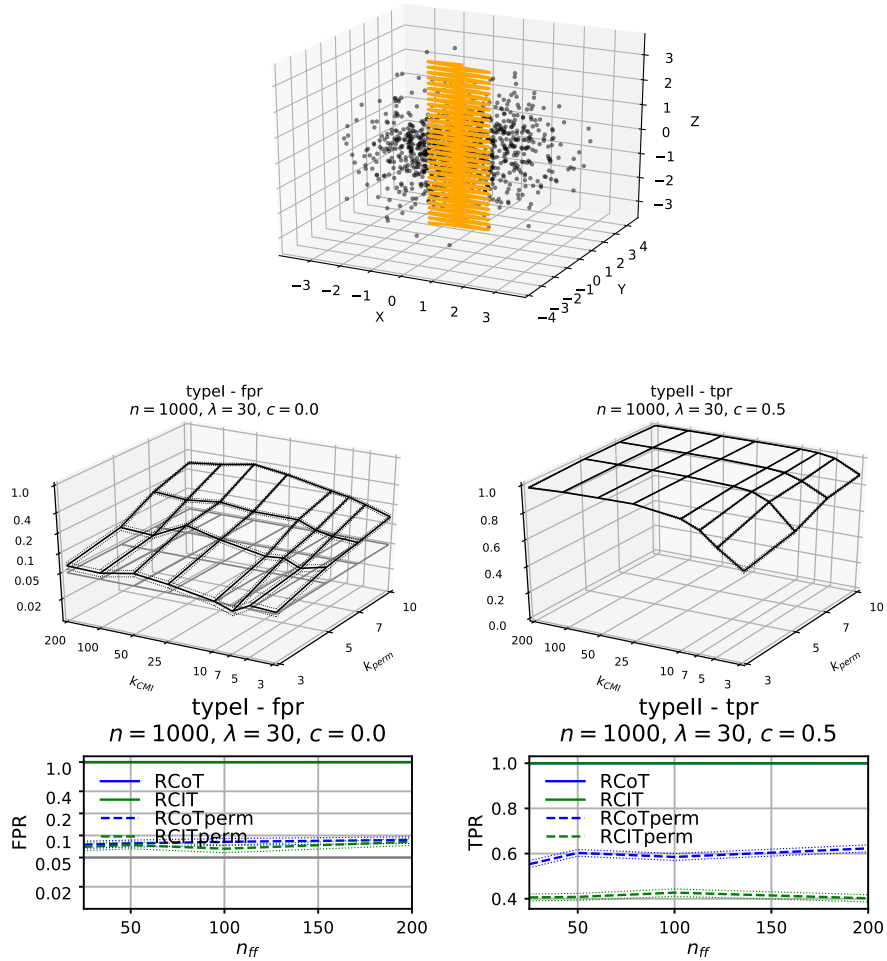


Figure 9: Example of sinusoidal dependence $X = \sin(\lambda Z) + \epsilon_X$ and $Y = \sin(\lambda Z) + \epsilon_Y$ leading to strongly oscillatory structure (top panel for $\lambda = 30$). The second row depicts FPR and TPR for CMiknn and the bottom row for RCIT and RCoT for different numbers of random features n_{ff} . Here the analytical versions of RCIT and RCoT (solid lines) do not work at all (FPR equal to 1). The permutation versions of RCIT and RCoT (dashed lines) use $k_{perm} = 5$.

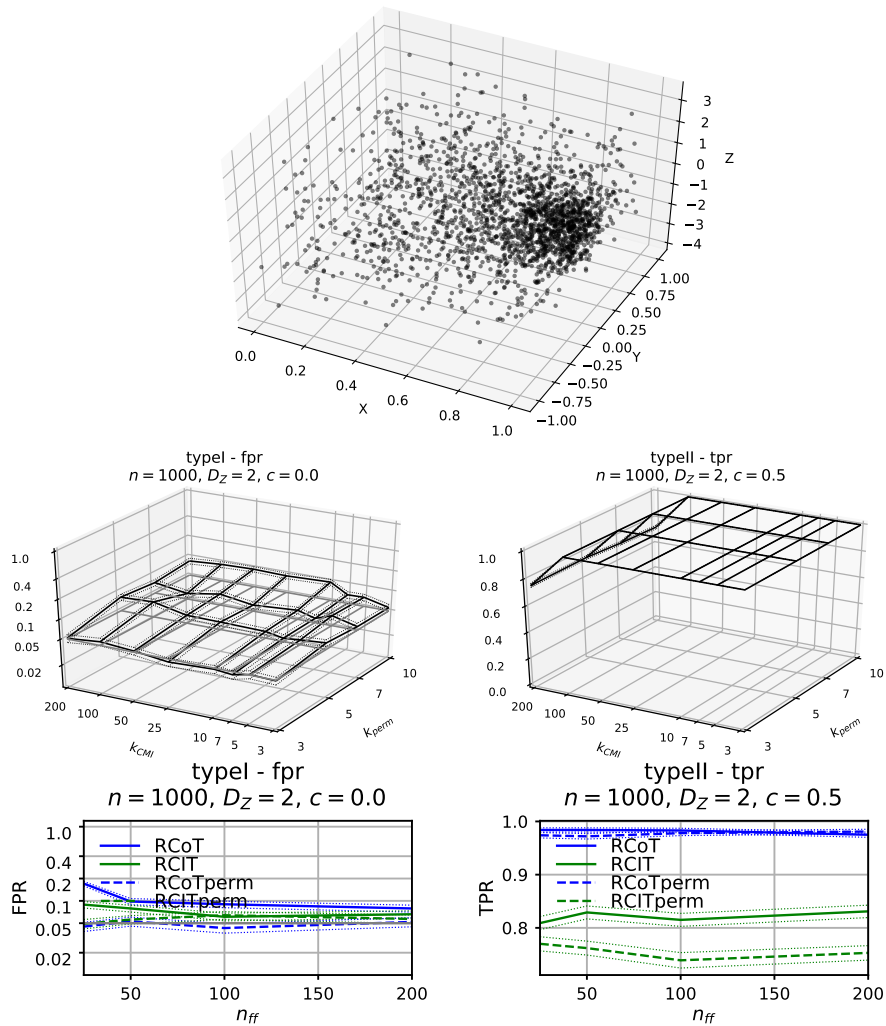


Figure 10: Example of multiplicative dependence of X and Y on Z leading to strongly nonlinear structure (top panel). Here the nearest-neighbor scheme of CMiknn can better adapt to the very localized density $D_Z = 2$ (center panel) with $k_{perm} < 7$ while RCIT and RCoT (bottom panel) do not well control false positives even if we resolve smaller scales better using a larger number of Fourier features n_{ff} . The permutation-versions are better calibrated, but have less power, especially RCIT.

Table 1: Results from Wang et al. (2015) together with results from RCoT and our CMI test. The experiments are described in Wang et al. (2015). Examples 1–4 correspond to conditional independence showing false positives and Examples 5–8 to dependent cases showing true positives at the 5% significance level. CMiknn was run with $k_{\text{CMI}} = 0.2n$ and $k_{\text{perm}} = 5, 10$. The numbers 50..250 denote the sample size.

Test	Example 1					Example 2				
	50	100	150	200	250	50	100	150	200	250
CDIT	0.035	0.034	0.05	0.057	0.048	0.046	0.053	0.055	0.048	0.058
CI.test	0.041	0.051	0.037	0.054	0.041	0.062	0.046	0.044	0.045	0.039
KCI.test	0.039	0.043	0.041	0.04	0.046	0.035	0.004	0.037	0.047	0.05
Rule-of-thumb	0.017	0.027	0.028	0.033	0.033	0.034	0.052	0.044	0.042	0.045
RCoT	0.074	0.059	0.055	0.043	0.050	0.056	0.056	0.069	0.055	0.073
CMiknn ($k_{\text{perm}} = 5$)	0.064	0.055	0.050	0.053	0.045	0.076	0.060	0.074	0.061	0.065
CMiknn ($k_{\text{perm}} = 10$)	0.058	0.061	0.057	0.058	0.046	0.075	0.066	0.053	0.057	0.071
Test	Example 3					Example 4				
	50	100	150	200	250	50	100	150	200	250
CDIT	0.035	0.048	0.055	0.053	0.043	0.049	0.054	0.051	0.058	0.053
CI.test	0.222	0.363	0.482	0.603	0.677	0.043	0.064	0.066	0.05	0.053
KCI.test	0.058	0.047	0.057	0.061	0.054	0.037	0.035	0.058	0.039	0.049
Rule-of-thumb	0.019	0.038	0.032	0.039	0.039	0.037	0.04	0.055	0.059	0.053
RCoT	0.074	0.047	0.046	0.053	0.054	0.115	0.072	0.066	0.061	0.053
CMiknn ($k_{\text{perm}} = 5$)	0.044	0.043	0.046	0.046	0.054	0.084	0.071	0.067	0.079	0.070
CMiknn ($k_{\text{perm}} = 10$)	0.063	0.065	0.061	0.076	0.067	0.101	0.113	0.106	0.098	0.084
Test	Example 5					Example 6				
	50	100	150	200	250	50	100	150	200	250
CDIT	0.898	0.993	1	1	1	0.752	0.995	1	1	1
CI.test	0.978	1	1	1	1	0.468	0.434	0.467	0.476	0.474
KCI.test	0.158	0.481	0.557	0.602	0.742	0.296	0.862	0.995	1	1
Rule-of-thumb	0.368	0.793	0.927	0.983	0.994	1	1	1	1	1
RCoT	0.817	0.986	0.998	1	1	0.301	0.533	0.679	0.807	0.860
CMiknn ($k_{\text{perm}} = 5$)	0.782	0.981	0.998	1	1	0.806	0.997	0.999	1	1
CMiknn ($k_{\text{perm}} = 10$)	0.855	0.995	1	1	1	0.805	0.995	1	1	1
Test	Example 7					Example 8				
	50	100	150	200	250	50	100	150	200	250
CDIT	0.918	0.998	1	1	1	0.361	0.731	0.949	0.977	0.994
CI.test	0.953	0.984	0.983	0.995	0.987	0.456	0.476	0.464	0.461	0.485
KCI.test	0.574	0.947	0.998	1	1	0.089	0.401	0.685	1	1
Rule-of-thumb	0.073	0.302	0.385	0.514	0.515	0.043	0.233	0.551	0.851	0.972
RCoT	0.594	0.880	0.962	0.985	0.991	0.275	0.392	0.470	0.624	0.654
CMiknn ($k_{\text{perm}} = 5$)	0.753	0.963	0.992	0.997	1	0.302	0.644	0.804	0.916	0.958
CMiknn ($k_{\text{perm}} = 10$)	0.798	0.976	0.999	0.999	0.999	0.323	0.680	0.832	0.920	0.971

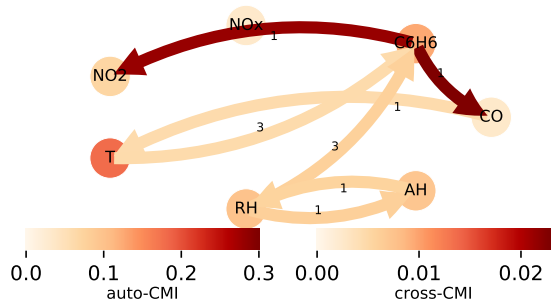


Figure 11: Causal discovery in time series of air pollutants and various weather variables. The node color gives the strength of auto-CMI and the edge color the cross-CMI with the link labels denoting the time lag in *hours*.

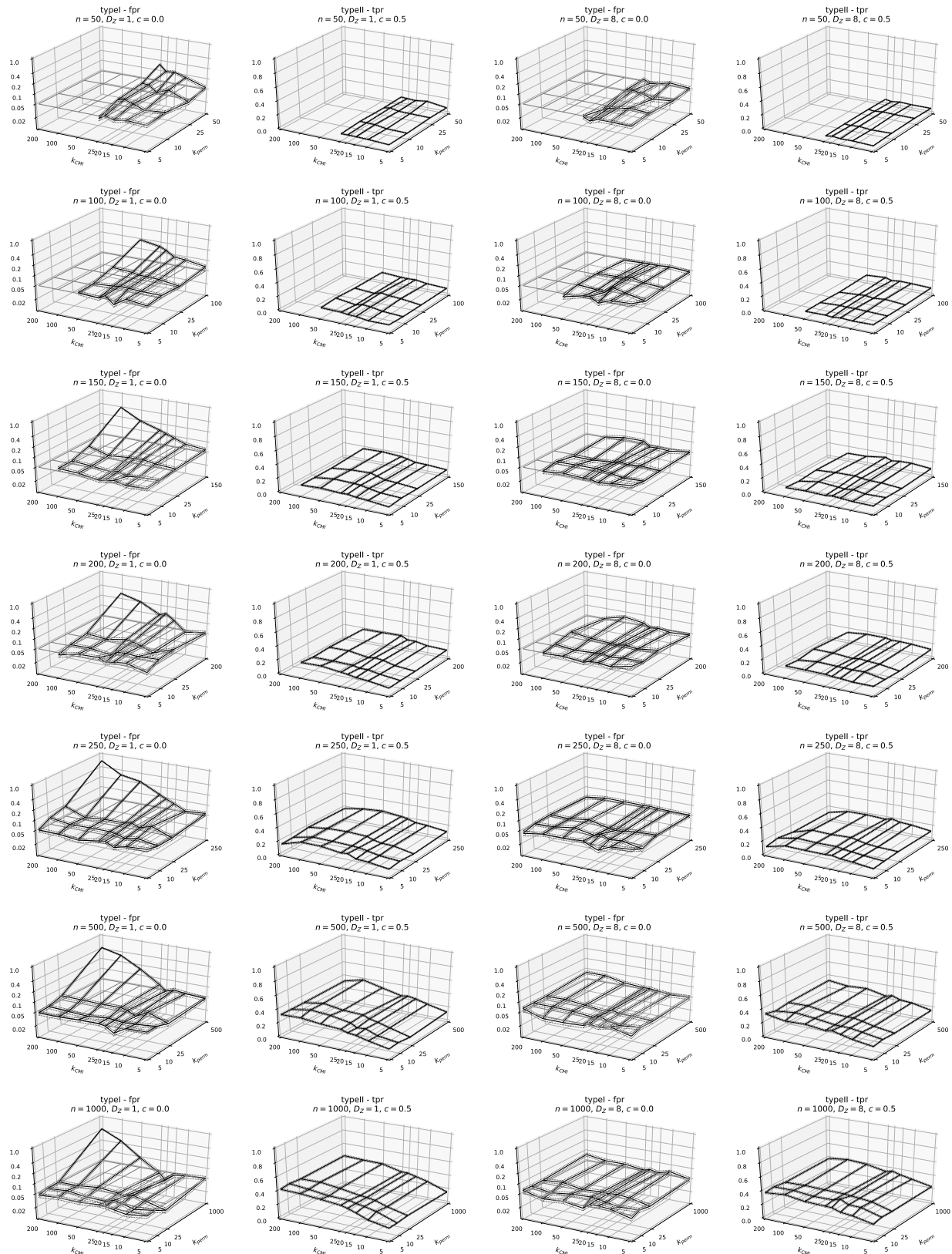


Figure 12: Same as in Fig. 3, but for more sample sizes from $n = 50$ (top) to $n = 1000$ (bottom).

Acknowledgements

We thank Eric Strobl for kindly providing R-code for KCIT, RCIT and RCoT and Dino Sejdinovic for many helpful comments.

References

- Bergsma, W. (2004). Testing conditional independence for continuous random variables. *Eurandom technical report*, 48:1–19.
- Daudin, J. J. (1980). Partial association and an measures to qualitative application regression. *Biometrika*, 67(3):581–590.
- De Vito, S., Massera, E., Piga, M., Martinotto, L., and Di Francia, G. (2008). On field calibration of an electronic nose for benzene estimation in an urban pollution monitoring scenario. *Sensors and Actuators, B: Chemical*, 129(2):750–757.
- Dobrushin, R. L. (1958). A simplified method of experimentally evaluating the entropy of a stationary sequence. *Theory of Probability & Its Applications*, 3(4).
- Doran, G., Muandet, K., Zhang, K., and Schölkopf, B. (2014). A Permutation-Based Kernel Conditional Independence Test. In *Proceedings of the Thirtieth Conference on Uncertainty in Artificial Intelligence*, pages 132–141.
- Frenzel, S. and Pompe, B. (2007). Partial Mutual Information for Coupling Analysis of Multivariate Time Series. *Physical Review Letters*, 99(20):204101.
- Fukumizu, K., Gretton, A., Sun, X., and Schölkopf, B. (2008). Kernel measures of conditional dependence. *Advances in neural information processing systems*, pages 489–496.
- Gao, W., Oh, S., and Viswanath, P. (2017). Demystifying fixed k-nearest neighbor information estimators. In *2017 IEEE International Symposium on Information Theory (ISIT)*, pages 1267–1271. IEEE.
- Goria, M. N. and Leonenko, N. N. (2005). A new class of random vector entropy estimators and its applications in testing statistical hypotheses. *Nonparametric Statistics*, 17(3):277–297.
- Huang, T. M. (2010). Testing conditional independence using maximal nonlinear conditional correlation. *Annals of Statistics*, 38(4):2047–2091.
- Kozachenko, L. F. and Leonenko, N. N. (1987). Sample estimate of the entropy of a random vector. *Problemy Peredachi Informatsii*, 23(2):9–16.
- Kraskov, A., Stögbauer, H., and Grassberger, P. (2004). Estimating mutual information. *Physical Review E*, 69(6):066138.
- Leonenko, N. N., Pronzato, L., and Savani, V. (2008). A class of Rényi information estimators for multidimensional densities. *The Annals of Statistics*, 36(5):2153–2182.
- Maneewongvatana, S. and Mount, D. (1999). It’s okay to be skinny, if your friends are fat. *Center for Geometric Computing 4th Annual Workshop on Computational Geometry*, pages 1–8.
- Margaritis, D. (2005). Distribution-free learning of Bayesian network structure in continuous domains. *Proceedings of the National Conference on Artificial Intelligence*, 20(2):825.
- Paparoditis, E. and Politis, D. N. (2000). The local bootstrap for kernel estimators under general dependence conditions. *Annals of the Institute of Statistical Mathematics*, 52(1):139–159.
- Peters, J. and Schölkopf, B. (2014). Causal Discovery with Continuous Additive Noise Models. *Journal of Machine Learning Research*, 15(June):2009–2053.
- Póczos, B. and Schneider, J. (2012). Nonparametric estimation of conditional information and divergences. *15th International Conference on Artificial Intelligence and Statistics*, XX:914–923.
- Ramsey, J. D. (2014). A Scalable Conditional Independence Test for Nonlinear, Non-Gaussian Data. <https://arxiv.org/abs/1401.5031>.
- Runge, J., Sejdinovic, D., and Flaxman, S. (2017). Detecting causal associations in large nonlinear time series datasets. <http://arxiv.org/abs/1702.07007>.
- Sejdinovic, D., Sriperumbudur, B., Gretton, A., and Fukumizu, K. (2013). Equivalence of distance-based and RKHS-based statistics in hypothesis testing. *The Annals of Statistics*, 41(5):2263–2291.
- Spirtes, P., Glymour, C., and Scheines, R. (2000). *Causation, Prediction, and Search*, volume 81. The MIT Press, Boston.
- Strobl, E. V., Zhang, K., and Visweswaran, S. (2017). Approximate Kernel-based Conditional Independence Tests for Fast Non-Parametric Causal Discovery. <http://arxiv.org/abs/1702.03877>.
- Vejmelka, M. and Paluš, M. (2008). Inferring the directionality of coupling with conditional mutual information. *Physical Review E*, 77(2):026214.
- Wang, Q., Kulkarni, S. R., and Verdú, S. (2009). Divergence Estimation for Multidimensional Densities Via k -Nearest-Neighbor Distances. *IEEE*

Transactions on Information Theory, 55(5):2392–2405.

Wang, X., Pan, W., Hu, W., Tian, Y., and Zhang, H. (2015). Conditional Distance Correlation. *Journal of the American Statistical Association*, 110(512):1726–1734.

Zhang, K., Peters, J., Janzing, D., and Schölkopf, B. (2012). Kernel-based conditional independence test and application in causal discovery. *preprint arXiv:1202.3775*.

Zhang, Q., Filippi, S., Flaxman, S., and Sejdinovic, D. (2017). Feature-to-Feature Regression for a Two-Step Conditional Independence Test. *Proceedings of the Thirtythird Conference on Uncertainty in Artificial Intelligence*.